UIVERSITY OF OSLO
Department of Informatics

Design of Capacity-Optimal High-Rank Line-of-Sight MIMO Channels

Research Report 352

Frode Bøhagen

Pål Orten

Geir E. Øien

Isbn 82-7368-309-5
Issn 0806-3036

March 2007

Design of Capacity-Optimal High-Rank Line-of-Sight MIMO Channels

Frode Bøhagen, Pål Orten, and Geir E. Øien

Abstract

This paper describes a technique for realizing a high-rank channel matrix in a *line-of-sight* (LOS) *multiple-input multiple-output* (MIMO) transmission scenario. This is beneficial for systems which are unable to make use of the originally derived MIMO gain given by *independent and identically distributed* (i.i.d.) flat Rayleigh fading channels. Typical applications are *fixed wireless access* (FWA) and radio relay systems. The technique is based on optimization of antenna placement in uniform linear arrays with respect to *mutual information* (MI) for pure LOS channels. Both the case where the channel is only known at the receiver and the case where the channel is known at the transmitter and receiver are treated. By introducing a new and more general 3-D geometrical model than that applied in earlier works, additional insight into the optimal design parameters is gained. We also perform a novel analysis of the sensitivity of the optimal design parameters, and derive analytical expressions for the eigenvalues in the pure LOS channel case, which are valid also when allowing for non-optimal design. Furthermore, we investigate the approximations introduced in the derivations, in order to reveal when the results are applicable, which turns out to be for most practical situations. The LOS transmission matrix is used in a Ricean fading channel model which incorporates spatial correlation between the non-LOS components, and performance is evaluated with respect to the average MI and the MI cumulative distribution function. Our results show that even with some deviation from the optimal design, the LOS MIMO scenario outperforms the i.i.d. Rayleigh scenario in terms of MI.

I. Introduction

Since the pioneering work of Foschini and Gans [1] and Telatar [2], *multiple-input multiple-output* (MIMO) systems have evolved into one of the most promising enabling technologies for resolving the problem of continued demand for increased bandwidth in wireless communications, and the technology is already hitting the market [3], [4]. The wireless frequency

spectrum is a very limited resource which must be utilized efficiently. MIMO systems can facilitate efficient frequency utilization by, among other things, smart signal processing at the *transmitter* (Tx) and *receiver* (Rx). An excellent tutorial report on progress in the area of wireless MIMO systems is presented in [5].

Most research efforts in the field of MIMO communications exploit the fading given by a multipath environment. Best performance for such a transmission scenario is assumed to be achieved for channels exhibiting *independent and identically distributed* (i.i.d.) frequency-flat Rayleigh fading between all Tx and Rx antennas [2]. In this paper we present a transmission scheme resulting in high MIMO gain also for channels which are not subject to severe multipath. Some work on this topic has also been performed by other authors. In [6] the possibility of enhancing performance by considering the array geometry when a strong LOS component is present is discussed. Furthermore, expressions for optimal placement of the antennas in parallel *uniform linear arrays* (ULAs) are introduced in [7], [8], [9], while some numerical investigations are presented in [10] and [11].

In this paper we give a more comprehensive presentation of the results we first presented in [12] and [13], where we propose a *3-D* geometrical model for the *line-of-sight* (LOS) component to be employed when applying ULAs at Tx and Rx. This model is used to find the optimal antenna separation with regard to *mutual information* (MI) for LOS channels, valid both when the channel is only known at the Rx, and when it is known at the Tx and Rx. The present paper extends work done by other authors on the topic by i) allowing the arrays to have arbitrary orientation in space[1], ii) characterizing how non-optimal design effects the system parameters, iii) giving analytical expressions for the eigenvalues of the pure LOS matrix, and iv) giving an analysis of the approximation required to get the analytical results. In contrast to the models used earlier ([7], [8], [9]), our model does not require the Tx and Rx arrays to be parallel. This results in additional insight into the optimal design parameters. As in [6], we will show that our scheme actually performs better for pure LOS channels than for i.i.d. Rayleigh channels. The theoretical results derived in this paper are supported by real world measurements reported in [11], [14], [15], [16], [17]. The solution will apply

[1]After we first presented our results on ULAs with arbitrary orientation in March 2005 [13], the same results have been reported by another research group in August 2006 [14].

nicely to *fixed wireless access* (FWA) (studied in [18]) and radio relay systems, as the optimal antenna spacing turns out to be a simple function of the Tx–Rx separation (which is fixed for such schemes), and since these systems often require a strong LOS component to function properly.

Furthermore, we introduce a *deviation factor* to perform an analysis of the sensitivity to non-optimal design, and derive analytical expressions for the eigenvalues for the pure LOS channel case as a function of this deviation factor. Moreover, we investigate the approximations introduced in the derivations, in order to reveal the scenarios to which the results are applicable. The performance of the transmission scheme is analyzed with respect to both the average MI and the MI *cumulative distribution function* (CDF), for different Ricean fading channels.

The remainder of the paper is organized as follows. Section II presents the MIMO system to be analysed, and discusses MI for MIMO channels. In Section III, MIMO channel models for the LOS and *non-LOS* (NLOS) cases are presented. Simulation and results for the presented scheme are given in Section IV, while conclusions are drawn in Section V.

II. THE MIMO SYSTEM

A wireless MIMO transmission system employs several Tx and Rx antennas when transmitting data over a channel. We denote the number of Tx antennas by N, while the number of Rx antennas is denoted M. Assuming slowly varying and frequency-flat fading channels, it is common to model the MIMO transmission in complex baseband as [5]

$$\mathbf{r} = \sqrt{\chi} \cdot \mathbf{H}\mathbf{s} + \mathbf{n}, \tag{1}$$

where $\mathbf{r} \in \mathbb{C}^{M\times 1}$ is the received signal vector, $\mathbf{s} \in \mathbb{C}^{N\times 1}$ is the transmitted signal vector, $\mathbf{H} \in \mathbb{C}^{M\times N}$ is the channel matrix, χ is the common power attenuation over the subchannels, and $\mathbf{n} \in \mathbb{C}^{M\times 1}$ is the *additive white Gaussian noise* (AWGN) vector. The elements of the channel matrix link the Rx antennas ($m \in \{0, 1, \ldots, M-1\}$) with the Tx antennas ($n \in \{0, 1, \ldots, N-1\}$). The additive noise vector contains i.i.d. circularly symmetric complex

Gaussian elements with zero mean and variance σ_n^2, i.e. $\mathbf{n} \sim \mathcal{CN}(\mathbf{0}_{M\times 1}, \sigma_n^2 \cdot \mathbf{I}_M)$[2], where $\mathbf{I}_M$ is the $M \times M$ identity matrix.

We assume that all the Rx antennas receive the same total average power from the desired signals, and that $\mathbf{H}$ is the *normalized* channel matrix, which implies that each element in $\mathbf{H}$ has unit average power. By introducing this normalization we make the average *signal-to-noise ratio* (SNR) independent of $\mathbf{H}$. We denote the total average received SNR at one Rx antenna $\bar{\gamma} = \frac{P \cdot \chi}{\sigma_n^2}$, where P is the total Tx power. For such a system, the MI of the MIMO transmission described by (1) can be expressed as [2][3]

$$\mathcal{I} = \sum_{i=1}^{U} \log_2 \left(1 + \bar{\gamma}_i \mu_i\right) \quad \text{bit/s/Hz}, \tag{2}$$

where $U = \min(M, N)$ and μ_i is the ith eigenvalue of $\mathbf{W}$ defined as

$$\mathbf{W} = \begin{cases} \mathbf{H}\mathbf{H}^H, & M \leq N \\ \mathbf{H}^H\mathbf{H}, & M > N, \end{cases} \tag{3}$$

where $(\cdot)^H$ is the Hermitian transpose operator. $\bar{\gamma}_i$ can be viewed as a power allocation factor which also contains the path loss and noise ('SNR allocation factor'), and is subject to the constraint

$$\bar{\gamma} = \sum_{i=1}^{N} \bar{\gamma}_i. \tag{4}$$

The transmission scheme employed is dependent on the available channel information. If the channel is only known at the Rx, we employ *equal power* (EP) transmission at Tx, i.e. $\bar{\gamma}_i = \frac{\bar{\gamma}}{N}$. In the case where the channel is known at both the Tx and the Rx, we employ the optimal power allocation scheme (capacity achieving) which follows the *waterfilling* (WF) principle [2], leading to the SNR expression

$$\bar{\gamma}_i = \left(\xi - \frac{1}{\mu_i}\right)_+, \tag{5}$$

where $(x)_+ \triangleq \max(0, x)$, and ξ is chosen to satisfy the constraint in (4).

[2]$\mathcal{CN}(\mathbf{x}, \mathbf{Y})$ denotes a circularly symmetric complex Gaussian distributed random vector, with mean vector $\mathbf{x}$ and covariance matrix $\mathbf{Y}$.

[3]Even though the derivation is different for the two transmission schemes investigated, i.e. EP allocation and WF power allocation, the MI for both cases can be expressed as in (2).

From (2) we see that the MI of a MIMO system can be viewed as the MI of U parallel *single-input single-output* (SISO) channels, where each channel has gain μ_i (given by the characteristics of $\mathbf{H}$) compared to a traditional SISO system with average SNR $\bar{\gamma}_i$.

III. MIMO CHANNEL MODEL

One way to model the channel matrix is as a sum of two components, a LOS component and a NLOS component. The ratio between the power of the two components gives the Ricean K-factor [19, p.52]. As discussed in Section II we want $\mathbf{H}$ to be normalized, and we can express the normalized channel matrix in terms of K as

$$\mathbf{H} = \sqrt{\frac{K}{1+K}} \cdot \mathbf{H}_{\text{LOS}} + \sqrt{\frac{1}{1+K}} \cdot \mathbf{H}_{\text{NLOS}}, \tag{6}$$

with the requirement $(\text{cov}(\text{vec}(\mathbf{H}_{\text{LOS}})))_{i,i} = (\text{cov}(\text{vec}(\mathbf{H}_{\text{NLOS}})))_{i,i} = 1 \ \forall \ i \in \{1, \ldots, MN\}$. Here $\text{vec}(\cdot)$ and $\text{cov}(\cdot)$ are the matrix vectorization (stacking the columns on top of each other) and covariance operator respectively, while $(\cdot)_{i,j}$ is used to specify the element in row i and column j in the matrix. The entries in the matrices are discussed in detail in the following two subsections.

A. LOS channel: Ray tracing

Here we concentrate on the pure LOS channel, and only the direct components between the Tx and Rx antennas. In [6], [7], [8], [9], [10], [11] it was shown that by placing the antennas in a MIMO system in a certain way, the pure LOS channel matrix actually becomes high rank[4], which corresponds to many non-zero eigenvalues μ_i, and thus high MI (cf. (2)). In this work we describe the geometry of the transmission scenario in a new and more general way, using two ULAs with arbitrary spatial orientation (not restricted to be parallel).

1) Optimal inter-antenna distance: Figure 1 illustrates the system to be analyzed. Due to the ULA assumption, the inter-antenna distances d_t and d_r, at the Tx and the Rx respectively, are constant over the arrays. d_t and d_r can however of course take different values. In the figure, the x-axis is taken to be in the direction from the lower end of the Tx array, which is

[4]The rank of a matrix is equal to the number of linearly independent rows (or columns) of the matrix, or equivalently the number of non-zero eigenvalues.

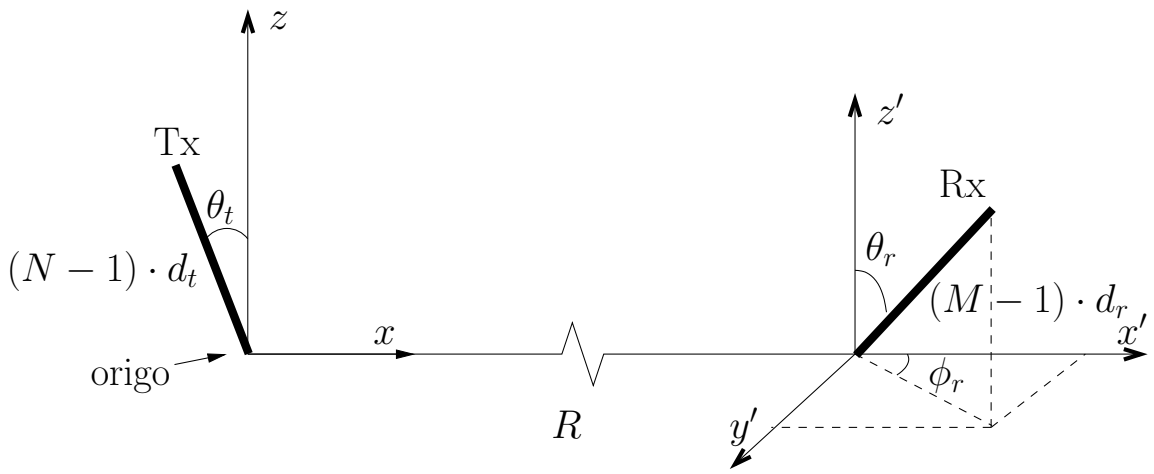

Fig. 1. A general MIMO system with ULAs at both the Tx and Rx. The Tx array is in the xz-plane with origo at the lower end, and the x-axis is from the lower end of the Tx array to the lower end of the Rx array.

origo, to the lower end of the Rx array. The Tx array is placed in the xz-plane. Furthermore, R represents the distance between the lower end of the arrays, $(N-1)\cdot d_t$ and $(M-1)\cdot d_r$ denote the total array lengths, and θ_t, θ_r, and ϕ_r are the angles of the local spherical coordinate system at the Tx and Rx. The figure can describe any MIMO system employing ULAs with arbitrary orientation.

The technique employed to model $\mathbf{H}_{\text{LOS}}$ is referred to as *ray-tracing* [6]. In this context, ray-tracing is based on finding the path length from each of the Tx antennas to each of the Rx antennas, and employing these path lengths to find the corresponding received phases. Consequently, the LOS channel is modeled by taking the true spherical nature of the wave propagation into account, i.e. no plane wave approximation. Only the direct component is considered (no reflections). We shall see later how these path lengths characterize $\mathbf{H}_{\text{LOS}}$, and thus its rank and MI.

First we need to define the vector $\mathbf{a}_n^t$ from origo to Tx antenna n, and the vector $\mathbf{a}_m^r$ from origo to Rx antenna m (the elements are ordered from element zero at the lower end of the arrays). Based on the parameters in Figure 1, we calculate the Euclidean norm of the vector difference between $\mathbf{a}_n^t$ and $\mathbf{a}_m^r$, to reveal the *path length* r_{mn} between Tx antenna n and Rx

antenna m:

$$\begin{aligned} r_{mn} &= \left\|\mathbf{a}_m^r - \mathbf{a}_n^t\right\| \\ &= \left[(R + md_r \sin\theta_r \cos\phi_r - nd_t \sin\theta_t)^2 + (md_r \sin\theta_r \sin\phi_r)^2\right. \\ &\quad \left. +(md_r \cos\theta_r - nd_t \cos\theta_t)^2\right]^{1/2} \qquad (7) \\ &\approx R + md_r \sin\theta_r \cos\phi_r - nd_t \sin\theta_t \\ &\quad + \frac{(md_r \sin\theta_r \sin\phi_r)^2 + (md_r \cos\theta_r - nd_t \cos\theta_t)^2}{2R} \qquad (8) \end{aligned}$$

In the last step above we made a Maclaurin series expansion [20, p.189] to the first order of the square root expression, i.e. $(1+\Delta)^{1/2} \approx 1 + \frac{\Delta}{2}$. This is a good approximation when $\Delta \ll 1$. We also approximated the denominator of the fraction in (8) by removing the terms representing the array lengths in the x-direction, which is valid when R is much larger than these lengths. Both approximations are thus valid simultaneously if the Tx–Rx distance R is much larger than the array dimensions at both the Tx and Rx.

We discuss the approximations, and their effect on the evaluation of the system performance in more detail in Appendix I. The main conclusion is that the approximations have little impact on the predicted MI as long as the angles θ_t and θ_r are small enough compared to the ratio between the array sizes and the Tx–Rx distance.

The symbols transmitted from Tx antenna n will be received at M different Rx antennas. The different path lengths over the Rx array corresponds to an inter-antenna phase difference. The channel response vector from Tx antenna n on the M Rx antennas can be written as

$$\mathbf{h}_n = \left[\exp\left(\frac{j2\pi}{\lambda} r_{0n}\right), \ldots, \exp\left(\frac{j2\pi}{\lambda} r_{(M-1)n}\right)\right]^T, \qquad (9)$$

where λ is the wavelength, each element is normalized as discussed earlier, and $(\cdot)^T$ denotes the vector transpose operator. The LOS channel matrix is thus given by $\mathbf{H}_{\text{LOS}} = [\mathbf{h}_0, \mathbf{h}_1, \ldots, \mathbf{h}_{N-1}]$.

We will now derive the optimal antenna separation, with regard to MI, for a pure LOS channel. In Appendix II we show that optimal values for μ_i, for both transmission scenarios, are obtained when all eigenvalues are equal, i.e. $\mu_i = V \ \forall\ i$, where $V = \max(M, N)$. One

realization of $\mathbf{W}$ which fulfills this requirement of equal eigenvalues is

$$\mathbf{W} = V \cdot \mathbf{I}_U. \tag{10}$$

From the definition of $\mathbf{W}$ in (3), we see that (10) is fulfilled when $\mathbf{H}_{\text{LOS}}$ has orthogonal columns for $M > N$, or orthogonal rows for $N \geq M$.

We will start by investigating the case where $M > N$, and generalizations to any combination of M and N will be made based on this result. Orthogonality between the different columns in $\mathbf{H}_{\text{LOS}}$ is obtained if the inner product between two channel response vectors from two different Tx antennas is equal to zero, i.e. $\langle \mathbf{h}_{n_1}, \mathbf{h}_{n_2} \rangle = 0 \ \forall \ n_1 \neq n_2$. Employing the expression for $\mathbf{h}_n$ from (9) and r_{mn} found in (8), the inner product can be expressed as

$$\begin{aligned} \langle \mathbf{h}_{n_1}, \mathbf{h}_{n_2} \rangle &= \sum_{m=0}^{M-1} \exp\left(\frac{j2\pi}{\lambda} \left(r_{mn_2} - r_{mn_1} \right) \right) \\ &= K^{(1)}_{n_1,n_2} \cdot \sum_{m=0}^{M-1} \exp\left(j2\pi \frac{d_t d_r \cos\theta_r \cos\theta_t}{\lambda R} \left(n_1 - n_2 \right) m \right), \end{aligned} \tag{11}$$

where

$$K^{(1)}_{n_1,n_2} = \exp\left(\frac{j2\pi}{\lambda} \left(d_t \sin\theta_t (n_1 - n_2) + d_t^2 \cos^2\theta_t (n_2^2 - n_1^2) \right) \right). \tag{12}$$

To simplify (11), we employ the expression for a finite geometric series [20, p.192] and trigonometric relations [20, p.127], and obtain the following orthogonality equation

$$\langle \mathbf{h}_{n_1}, \mathbf{h}_{n_2} \rangle = K^{(1)}_{n_1,n_2} \cdot K^{(2)}_{n_1,n_2} \cdot \frac{\sin\left(\pi \frac{d_t d_r}{\lambda R} \cos\theta_r \cos\theta_t (n_1 - n_2) M \right)}{\sin\left(\pi \frac{d_t d_r}{\lambda R} \cos\theta_r \cos\theta_t (n_1 - n_2) \right)} = 0, \tag{13}$$

where

$$K^{(2)}_{n_1,n_2} = \exp\left(j\pi \frac{d_t d_r \cos\theta_r \cos\theta_t}{\lambda R} \left(n_1 - n_2 \right) \left(M - 1 \right) \right). \tag{14}$$

Since $|K^{(1)}_{n_1,n_2} \cdot K^{(2)}_{n_1,n_2}| = 1$, it does not contribute to the solution of (13). The solution is found when the $\sin(\cdot)$ in the numerator is zero without the $\sin(\cdot)$ in the denominator being zero, which can be expressed mathematically as

$$d_t d_r \in \left\{ \frac{\lambda R}{M \cos\theta_r \cos\theta_t} \cdot \upsilon_1 \right\} \setminus \left\{ \frac{\lambda R}{\cos\theta_r \cos\theta_t} \cdot \frac{\upsilon_2}{n_1 - n_2} \right\}, \tag{15}$$

where $\upsilon_1, \upsilon_2 \in \mathbb{Z}$, and "\" is the set difference operator[5]. In (15), we have chosen the key design parameter to be the product between d_t and d_r, from now on referred to as the *antenna separation product* (ASP). The optimal ASP in (15) depends on the wavelength, Tx–Rx distance, the number of Rx antennas, θ_t and θ_r. Furthermore, we see that optimal design is achieved when υ_1 is chosen to satisfy the relation $\frac{\upsilon_1(n_1-n_2)}{M} \notin \mathbb{Z}$.

The above result can easily be generalized to any combination of M and N, by realizing that a similar result can be obtained for $N \geq M$. In this case the rows of $\mathbf{H}_{\text{LOS}}$ must be orthogonal to fulfill (10). The derivation follows a similar procedure, and the only difference in the result is that M becomes N in (15), i.e., the general solution is found by swapping M with V in (15). The solution corresponding to the smallest ASP is probably the most interesting from a practical design point of view, because it requires the shortest antenna arrays. This solution is given by choosing $\upsilon_1 = 1$, which always is optimal because $V > 1$ and thus $\frac{\upsilon_1(n_1-n_2)}{V} \notin \mathbb{Z}$ (remember that $(n_1 - n_2) \in \{\pm 1, \ldots, \pm(V-1)\}$). The optimal ASP with respect to MI for ULAs therefore becomes

$$d_t d_r = \frac{\lambda R}{V \cos\theta_t \cos\theta_r}. \tag{16}$$

In practical scenarios, λ, V, and R may be given, whereas the system designer may jointly optimize values of d_t, d_r, θ_t, and θ_r. Comparing (16) to what was found in [7, Eq. (4)] and [8, Eq. (5)], which are valid only for parallel antenna arrays, we see that if we have $\theta_t = 0^\circ$ and $\theta_r = 0^\circ$ (parallel arrays) the same result is obtained. Equation (16) is thus a more general result which supports any orientation of the Tx and Rx arrays. Another important new insight from the general model is that the optimal ASP is independent of the rotation angle, ϕ_r, from Figure 1.

An interesting observation is that if we project the antenna arrays along the local z-axes at the Tx and Rx sides in Figure 1, and use the new antenna separation distances $d_t \cos\theta_t$ and $d_r \cos\theta_r$ for the parallel array solutions in [7] and [8], we actually get the same result as in (16)[6]. It is easy to verify that this projection model is not exact. However, from (16) it is clear that the result is the same, and thus this equivalence must simply be a consequence

[5] $x \in A \setminus B$ is defined as $\{x \in A \text{ and } x \notin B\}$

[6] Actually, this was the procedure we employed to derive (16) in [12].

of the approximations performed in our derivations.

By inspection of (16) it can be observed that LOS MIMO systems are best suited for applications where the transmission distance is constant, such as for example FWA and radio relay systems. Further, we see that the optimal ASP is proportional to λR, thus to prevent too large antenna arrays, the scheme is best suited for short range communications and/or high frequency applications. As an example, a 2×2 MIMO system, operating at 40 GHz with Tx–Rx distance 500 m and parallel arrays, achieves optimal design if $d_t d_r = 1.875$ m^2, e.g. if both arrays have length 1.37 m. However, for FWA systems it would probably be more practical to have a larger antenna separation at the base station than the subscriber unit, i.e. $d_t \neq d_r$.

2) Sensitivity to non-optimal design: A natural question to ask is, what happens if the parameters deviate from the optimal relation given in (16)? In the analysis to follow we investigate how sensitive the performance of ULA based LOS MIMO is to such deviations. For this purpose we introduce a *deviation factor*, denoted η, defined as the ratio between the optimal ASP, i.e. RHS of (16), and the actual ASP,

$$\eta \triangleq \frac{\text{ASP}_{\text{opt}}}{\text{ASP}} = \frac{\lambda R}{d_t d_r V \cos\theta_t \cos\theta_r}. \tag{17}$$

From this definition we see that if η is larger than unity, the actual ASP is too small compared to the optimal, while an η smaller than one indicates that the actual ASP is too large.

The influence of non-optimal design on $\mathbf{W}$, is that the eigenvalues start to deviate from optimal. In Appendix III we describe a procedure to find these eigenvalues. The procedure is based on the approximate path length from (8). The eigenvalues for $U = 2$ as a function of η, are given by

$$\mu_1^a = V + \frac{\sin\left(\frac{\pi}{\eta}\right)}{\sin\left(\frac{\pi}{V\eta}\right)} \quad \text{and} \quad \mu_2^a = V - \frac{\sin\left(\frac{\pi}{\eta}\right)}{\sin\left(\frac{\pi}{V\eta}\right)}, \tag{18}$$

where μ_i^a denotes the eigenvalues found by applying the approximate path length. For $U = 3$,

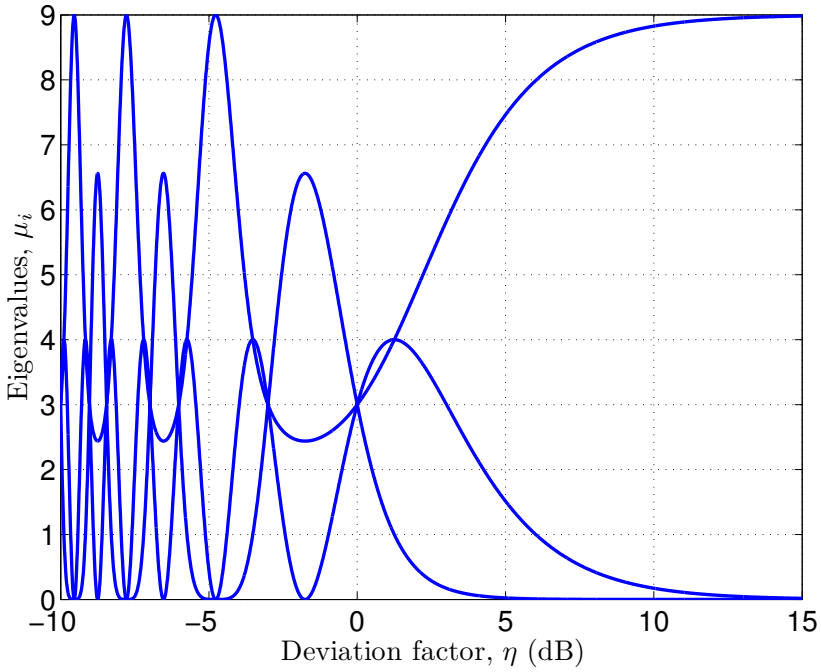

Fig. 2. $\{\mu_i\}$ for a 3×3 MIMO system as a function of η in dB when $\mathbf{H} = \mathbf{H}_{\text{LOS}}$.

we get the eigenvalues

$$\mu_1^a = V + \frac{\sin\left(\frac{2\pi}{\eta}\right) + 2\sin\left(\frac{\pi}{\eta}\right)\sqrt{\cos^2\left(\frac{\pi}{\eta}\right) + 8\cos^2\left(\frac{\pi}{\eta V}\right)}}{2\sin\left(\frac{2\pi}{\eta V}\right)}, \tag{19}$$

$$\mu_2^a = V - \frac{\sin\left(\frac{2\pi}{\eta}\right)}{\sin\left(\frac{2\pi}{\eta V}\right)}, \text{ and} \tag{20}$$

$$\mu_3^a = V + \frac{\sin\left(\frac{2\pi}{\eta}\right) - 2\sin\left(\frac{\pi}{\eta}\right)\sqrt{\cos^2\left(\frac{\pi}{\eta}\right) + 8\cos^2\left(\frac{\pi}{\eta V}\right)}}{2\sin\left(\frac{2\pi}{\eta V}\right)}. \tag{21}$$

By inspection we see, in both cases, that all eigenvalues are equal to V when $\eta = 1$ for these MIMO systems. This agrees well with what is stated in Appendix II: $\sum_i \mu_i = U \cdot V$, and optimal performance is achieved when $\{\mu_i\}_{i=1}^{U} = V$. The optimal power allocation scheme with respect to MI is EP in this case, and from (2) we observe that the MI becomes greater than or equal to U times the SISO MI with the same P.

As an example of the eigenvalue spread, we have plotted the eigenvalues $\{\mu_i^a\}_{i=1}^{3}$ as a function of η for a 3×3 pure LOS channel in Figure 2, i.e. (19)–(21) with $V = 3$. The figure

shows that the optimum (i.e., $\mu_i = 3$) is obtained for $\eta = 0$ dB, and periodically for smaller η. The explanation for this periodic behavior is that (15) has more than one solution, as discussed earlier. As already stated we concentrate on the solution corresponding to $\eta = 0$ dB because this gives the smallest ASP, implying smallest array sizes. By examining Figure 2 together with (2) we get an intuitive picture on how the deviation from optimal design values influences the MI for a pure LOS 3×3 MIMO system. This relation will be studied in more detail in Section IV.

3) Some comments on the deviation factor: There can be several reasons for η to deviate from 0 dB. For example, the optimal ASP may be too large for practical systems so that a compromise is needed, or the parameters in (16) may be difficult to determine with sufficient accuracy. A third reason might be wavelength dependency. A communication system always occupies a non-zero bandwidth, while the antenna distance can only be optimal for one single frequency. As an example consider the 10.5 GHz licensed band (10.000 - 10.680 GHz [21]). If we design a system for the center frequency, the deviation for the lower frequency yields $\lambda_{\text{low}}/\lambda_{\text{design}} = f_{\text{design}}/f_{\text{low}} = 10.340/10.000 = 1.034 = 0.145$ dB. Thus for the 3×3 system, this has only a small contribution to η, and thus little impact on the performance (see Figure 2).

B. NLOS channel

The NLOS channel matrix in the Rice model from (6) is a result of reflections, diffraction, and scattering from the transmission environment. This component is stochastic, and can be described by statistical models. In the analysis we want to include the effect of spatial correlation between the antenna elements, which often is due to insufficient antenna spacing, existence of a few dominant scatterers and small *angle-of-arrival* spreading. Spatial correlation usually results in rank deficiency, and thus reduces the MI. We model $\mathbf{H}_{\text{NLOS}}$ by the Kronecker model as [5]

$$\mathbf{H}_{\text{NLOS}} = (\mathbf{R}_r)^{1/2}\mathbf{H}_w(\mathbf{R}_t)^{1/2}, \tag{22}$$

where $\text{vec}(\mathbf{H}_w) \sim \mathcal{CN}(\mathbf{0}_{MN\times 1}, \mathbf{I}_{MN})$, and $\mathbf{R}_r \in \mathbb{C}^{M\times M}$ and $\mathbf{R}_t \in \mathbb{C}^{N\times N}$ are the local correlation matrices at the Rx and Tx respectively. For the model in (22) we have $\text{cov}(\text{vec}(\mathbf{H}_{\text{NLOS}})) = \mathbf{R}_r \otimes \mathbf{R}_t$, where $\otimes$ is the Kronecker product [5].

We further model the correlation as exponential [22], i.e. the correlation decays exponentially with the antenna separation, which is a physically realistic model for ULAs [23]. The elements of the Rx correlation matrix is then given by

$$(\mathbf{R}_r)_{i,j} = \begin{cases} \rho_r^{j-i} & i \leq j \\ (\rho_r^*)^{i-j} & i > j \end{cases} \qquad |\rho_r| \leq 1, \quad i,j \in \{1,\ldots,M\}, \tag{23}$$

where x^* is the complex conjugate of x, and ρ_r is the correlation coefficient between two neighboring Rx antennas ($\mathbf{R}_t$ is given in a similar way).

We can identify some connections between the optimal design parameters in (16) for LOS channels and the severity of the spatial NLOS correlation quantified by ρ. First of all an increase in the antenna separation d_t or d_r is usually beneficial with regards to spatial correlation, because the correlation function is typically a decreasing function with distance [19, p.67]. Further, when the transmission frequency increases (i.e. decreasing λ) the multipath usually decreases, resulting in increased spatial correlation. This is due to the fact that the path loss increases, which reduces the number of significant multipath components received. Of course there are also other parameters that influence the correlation which is not part of (16), as e.g. the number of scatterers in the transmission environment and the properties of the antennas employed. We observe that if $\rho = 0$ (no correlation), we get $\mathbf{R}_t = \mathbf{I}_N$ and $\mathbf{R}_r = \mathbf{I}_M$, thus $\mathbf{H}_{\text{NLOS}}$ becomes an i.i.d. Rayleigh channel in this case.

IV. Simulations and results

When the channel is stochastic, as in the case of $K \neq \infty$ dB, the MI given by (2) in Section II becomes a random variable. We employ the average MI and the MI CDF to characterize this random behavior. Average MI is the mean MI over all channel realizations for a specific average SNR, i.e. $\bar{\mathcal{I}} = E[\mathcal{I}(\bar{\gamma})]$, where $E[\,\cdot\,]$ is the expectation operator. Further, the MI CDF is given by $F_{\mathcal{I}}(\nu) = \Pr[\mathcal{I} \leq \nu]$.

The example system analyzed in this section is a 3×3 MIMO system. When investigating the performance of this system it may be convenient to look at the extremal points, since in practice we will lie somewhere in between these points. For instance, from (6) we see that $K = -\infty$ dB gives a NLOS channel matrix, while $K = \infty$ dB gives a pure LOS channel. Likewise, $\eta = 0$ dB gives optimal ASP, while $\eta = 30$ dB approximates a total antenna

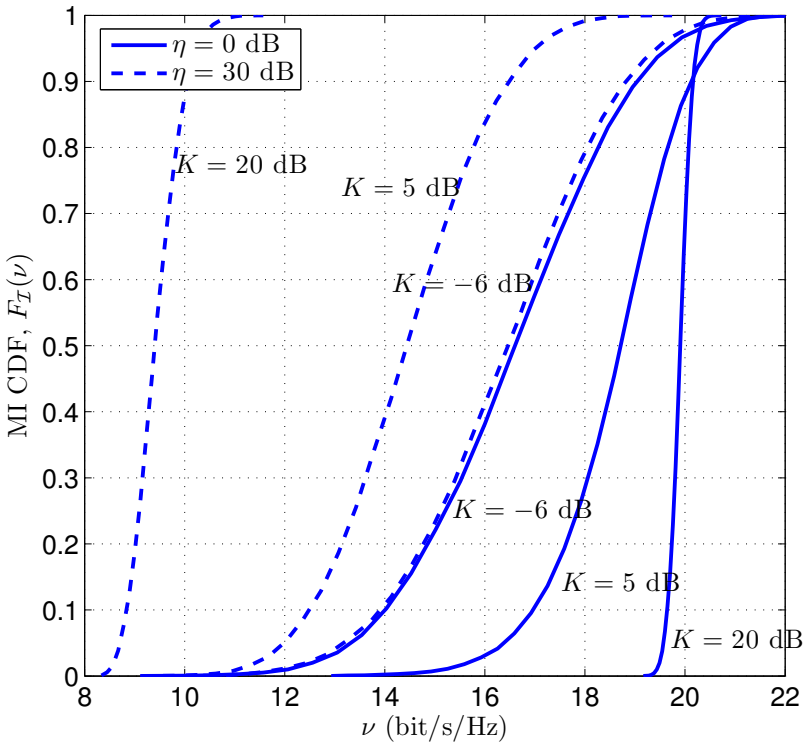

Fig. 3. $F_{\mathcal{I}}(\nu)$ for a 3×3 EP allocation MIMO system with $\bar{\gamma} = 20$ dB, different deviation factors η, no NLOS correlation, and different values of the Ricean K-factor.

separation mismatch ($\text{rank}(\mathbf{H}_{\text{LOS}}) = 1$, cf. Figure 2). It is important to note that when we use the term optimal design in this paper it is the relation given in (16), which is optimal for the pure LOS channel and not necessarily the general Ricean channel. If nothing else is mentioned, no NLOS correlation is assumed, i.e. $\rho_t = \rho_r = 0$.

Figure 3 shows $F_{\mathcal{I}}(\nu)$ for the system when employing EP transmission. Two different scenarios are illustrated, optimal design and total design mismatch. We observe how $F_{\mathcal{I}}(\nu)$ for the two situations become equal when the Ricean K-factor decrease and the channel matrix approaches a pure Rayleigh matrix. This is as expected because when $K = -\infty$ dB, the channel is independent of $\mathbf{H}_{\text{LOS}}$. When K increases, the MI increases towards its maximum, $U \cdot \log_2(1 + \frac{\bar{\gamma}}{N}V)$, for $\eta = 0$ dB. However, it decreases for η = 30 dB towards $\log_2(1 + M\bar{\gamma})$. This shows that LOS channels with optimal ASP is superior in terms of $F_{\mathcal{I}}(\nu)$ compared to MIMO systems based on i.i.d. Rayleigh channels. From the figure we see that the MI has some remaining stochastic behavior for $K = 20$ dB ($F_{\mathcal{I}}(\nu)$ is not a perfect step function). This figure is similar to one of the figures given in [6], where only

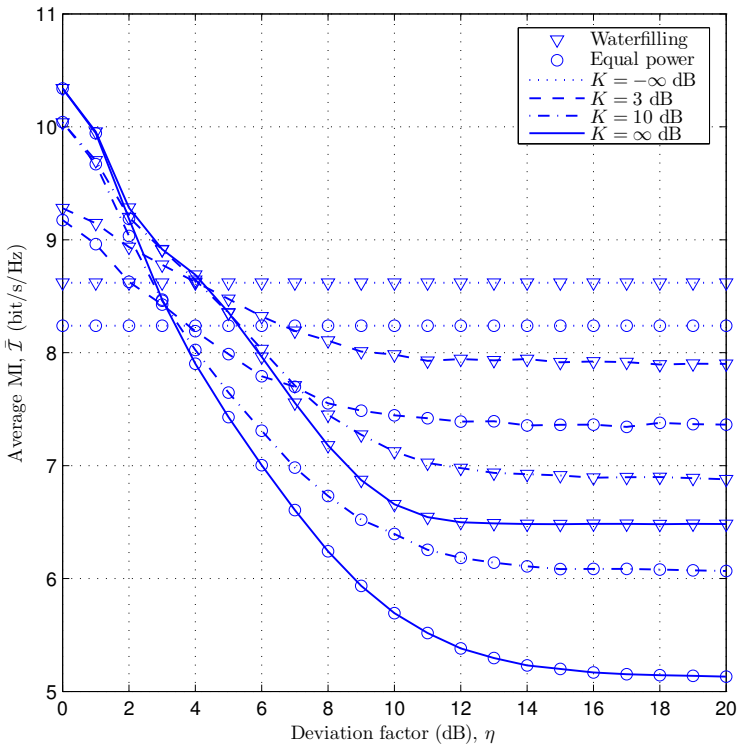

Fig. 4. $\bar{\mathcal{I}}$ for a 3×3 MIMO system both for EP allocation and WF power allocation as a function of η, with $\bar{\gamma}$ = 10 dB, no NLOS correlation, and different Ricean K-factors.

the extreme cases were investigated ($\text{rank}(\mathbf{H}_{\text{LOS}}) = 1$ and $\text{rank}(\mathbf{H}_{\text{LOS}}) = 3$). In what follows we will investigate how sensitive the MI for this system is to deviations from optimal ASP, by allowing η to have values between its extremal values.

In Figure 4 we have plotted $\bar{\mathcal{I}}$ for the system for both EP allocation and WF power allocation as a function of η. This is done for different values of the Ricean K-factor to see how $\bar{\mathcal{I}}$ is influenced by these variables. In both cases the figure shows that as K increases the system becomes increasingly dependent on η. When $K = -\infty$ dB, $\bar{\mathcal{I}}$ is independent of η as expected. It is also interesting to note that for EP transmission, at $\eta \approx 3$ dB, $\bar{\mathcal{I}}$ is almost independent of K, while for WF power allocation the same situation occurs for $\eta \approx 4$ dB. Additional investigation shows that this point seems to be relatively fixed for different values of $\bar{\gamma}$. For higher channel matrix dimensions however, the point will not be as well defined (the crossings of $K = -\infty$ dB are more spread). The figure also illustrates nicely the difference between the EP allocation and the WF power allocation scheme. In the case of equal eigenvalues, i.e. $\eta = 0$ dB and $K = \infty$ dB, the performance is equal for the two

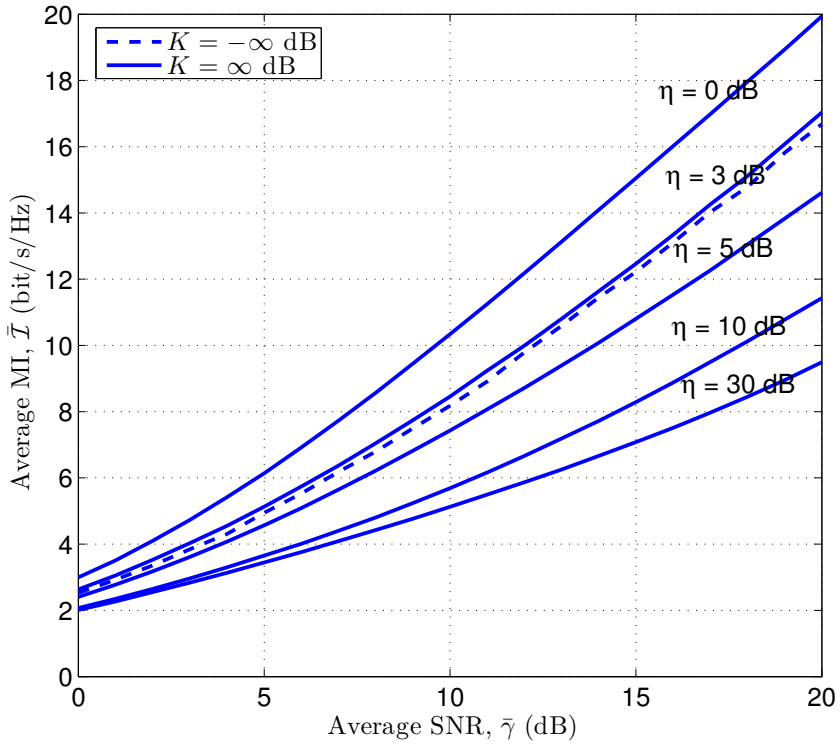

Fig. 5. $\bar{\mathcal{I}}$ for a 3×3 EP transmission MIMO system. Solid lines are for $K = \infty$ dB with different values of η in dB. The dotted line is for $K = -\infty$ dB with no NLOS correlation.

schemes and EP allocation is optimal, but as the eigenvalues spread we get increasing benefit from utilizing the WF scheme.

Figure 5 shows $\bar{\mathcal{I}}$ for the system under investigation with EP transmission as a function of $\bar{\gamma}$. The figure illustrates how $\bar{\mathcal{I}}$ decreases as η increases for pure LOS channels. This figure also confirms that these channels perform better than i.i.d. Rayleigh channels with respect to MI when doing optimal antenna spacing. We can also verify that when $\eta \approx 3$ dB for $K = \infty$ dB, we get almost the same performance as for i.i.d. Rayleigh channels.

The effect of spatial correlation between the NLOS components on $\bar{\mathcal{I}}$ is illustrated in Figure 6. The main contribution of the correlation is that it reduces the average MI for strong NLOS channels. For strong LOS channels, i.e. large K-factors, the MI is independent of the NLOS correlation. Consequently, the MI gap between optimal design pure LOS channels and pure NLOS channels increases when the correlation increases. For the optimal design case, we see that it is first when the $K < 0$ dB that the correlation has any noticeable influence on the MI, while for $\eta = 30$ dB this occurs for much larger K-factors.

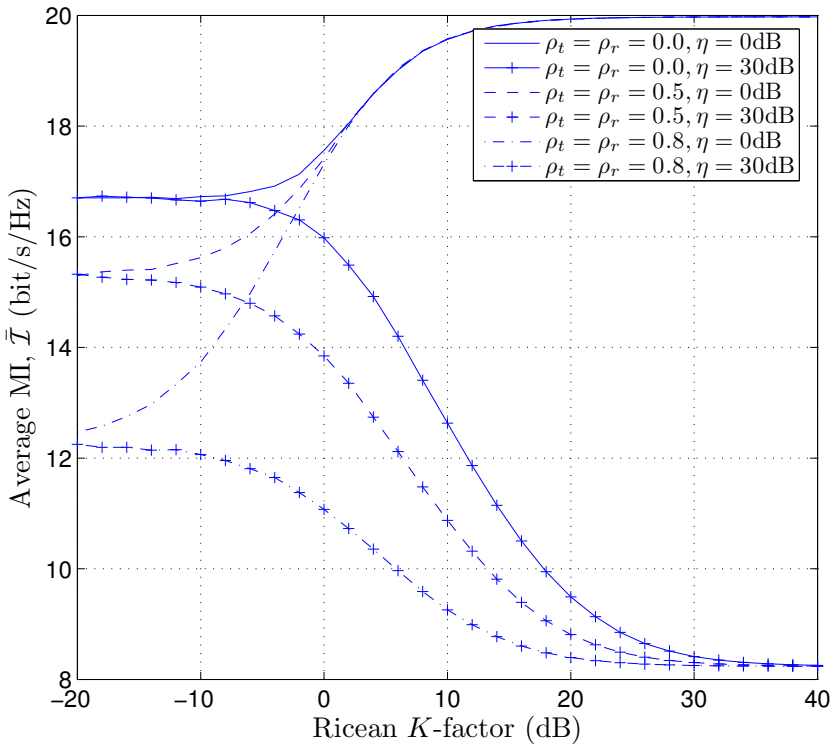

Fig. 6. $\bar{\mathcal{I}}$ for a 3×3 EP transmission MIMO system for different array design and correlation situations, with $\bar{\gamma} = 20$ dB.

In Figure 7 we have illustrated the MI gain by employing WF power allocation (instead of EP allocation), for the system transmitting over a pure LOS channel. From the figure we see that the gain increases as η increases as expected, because it results in a larger eigenvalue spread. The stepwise increase in relative MI gain is due to the fact that in the WF case $\bar{\mathcal{I}}$ decreases with η in a stepwise manner, each step starts when the number of active channels is reduced by one. Since we are investigating a 3×3 system we get two such steps. Further, in accordance with [5], WF power allocation gives the highest MI gain when $\bar{\gamma}$ is small. The extra complexity introduced by employing WF power allocation results in insignificant MI gain when η is below 0.5 dB, 1 dB, 4 dB, and 6 dB, for $\bar{\gamma}$ equal to 5 dB, 10 dB, 20 dB, and 30 dB respectively.

V. Conclusions

We have presented and optimized performance results for a general 3-D geometrical model for LOS MIMO channels, allowing for arbitrary orientation of the Tx and Rx arrays. The new model is utilized to derive the optimal *antenna separation product* (ASP) for *uniform*

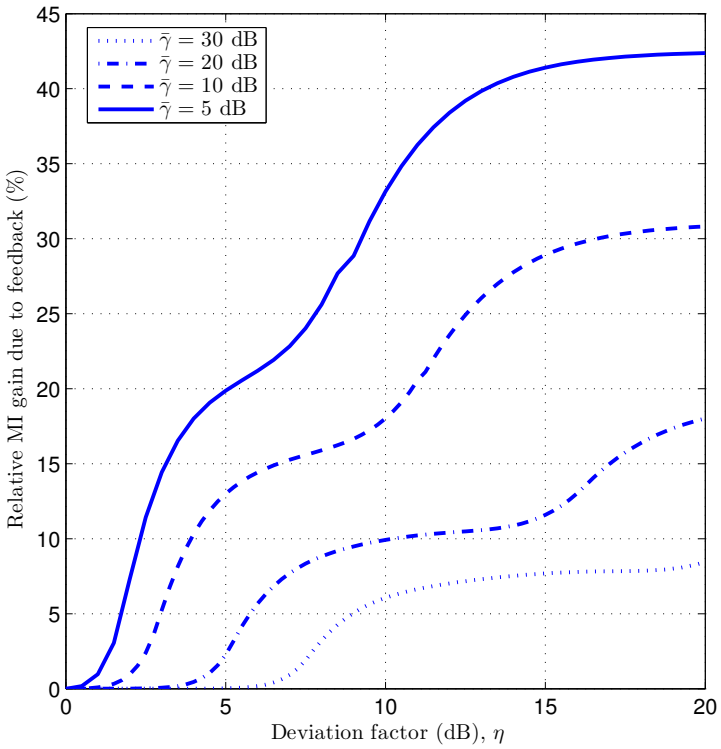

Fig. 7. Relative MI gain due to employing WF power allocation compared to EP transmission as a function of η in dB, for a 3×3 MIMO system with $K = \infty$ dB, and different $\bar{\gamma}$.

linear arrays (ULAs) with respect to MI for this pure LOS channel. Both the case where the channel is only known at the Rx, and when it is known both at the Tx and the Rx are treated. The ASP becomes a simple function of Tx–Rx separation, wavelength, dimension of the MIMO system, and the spherical angles at the local coordinate systems at the Tx and Rx. Another important result of the optimal design is the independence with respect to the rotation angle. The result is useful both for system designers when designing MIMO systems that are subject to strong LOS components, and when investigating the performance of such systems.

When we use optimal ASP, the MIMO transmission system performs better in terms of MI for pure LOS channels than for i.i.d. Rayleigh channels. When including spatial NLOS correlation, this MI gap between pure LOS and pure NLOS channels increases further. For the 3×3 system investigated in Section IV, we can tolerate an ASP of half the optimal value before the average MI degrades to that of the i.i.d. Rayleigh case. Investigating the approximations performed, we found that the results presented in this paper are applicable

when the spherical angels θ_t and θ_r are small enough compared to the ratio between the antenna array sizes and the distance between the Tx and Rx.

APPENDIX I
EVALUATION OF THE APPROXIMATION ERROR

Introducing the distance approximations in (8) makes it possible to derive an expression for the optimal ASP in Section III-A.1, and analytical expressions for the eigenvalues in the pure LOS case in Appendix III. In itself, this distance approximation is good if the distance between the lower end of the arrays is much larger than the array dimensions at both sides of the radio link. But, the distance approximation error will carry over to the later expressions, and eventually affect the LOS channel matrix characteristics. A framework for analyzing the MI error introduced by this approximations is presented here.

Both for the exact and the approximate path length in (7) and (8) respectively, it is straightforward to reformulate the phase expressions in (9) (the arguments of the exponential functions) as functions of the parameters $\frac{\lambda}{R}$, $\frac{d_t}{R}$, $\frac{d_r}{R}$, θ_t, θ_r, and ϕ_r. By using these parameters in the following inspection we make the results more general. Since η is an important parameter in this work we also want to include it in this investigation. This is achieved by rewriting (17) as

$$\frac{\lambda}{R} = \eta V \frac{d_t}{R}\frac{d_r}{R}\cos\theta_t \cos\theta_r, \tag{24}$$

which is employed in (7) and (8) to exchange $\frac{\lambda}{R}$ with η.

The error measure used is the relative MI error, which we define as the absolute value of the difference between the MI given by employing exact eigenvalues (found numerically), $\mathcal{I}^e$, and the MI predicted with the approximations, $\mathcal{I}^a$, divided by $\mathcal{I}^e$, i.e.

$$\varepsilon = \left|\frac{\mathcal{I}^e - \mathcal{I}^a}{\mathcal{I}^e}\right| = \left|1 - \frac{\sum_{i=1}^{U}\log_2\left(1+\bar{\gamma}_i\mu_i^a\right)}{\sum_{i=1}^{U}\log_2\left(1+\bar{\gamma}_i\mu_i^e\right)}\right|, \tag{25}$$

where μ_i^e is the exact eigenvalues. For $U = 2$ and $U = 3$, $\{\mu_i^a\}_{i=1}^{U}$ are given in Section III-A.2.

The framework for analyzing the approximation error described here includes many free variables, and a simple answer to when the approximation is valid is difficult to find.

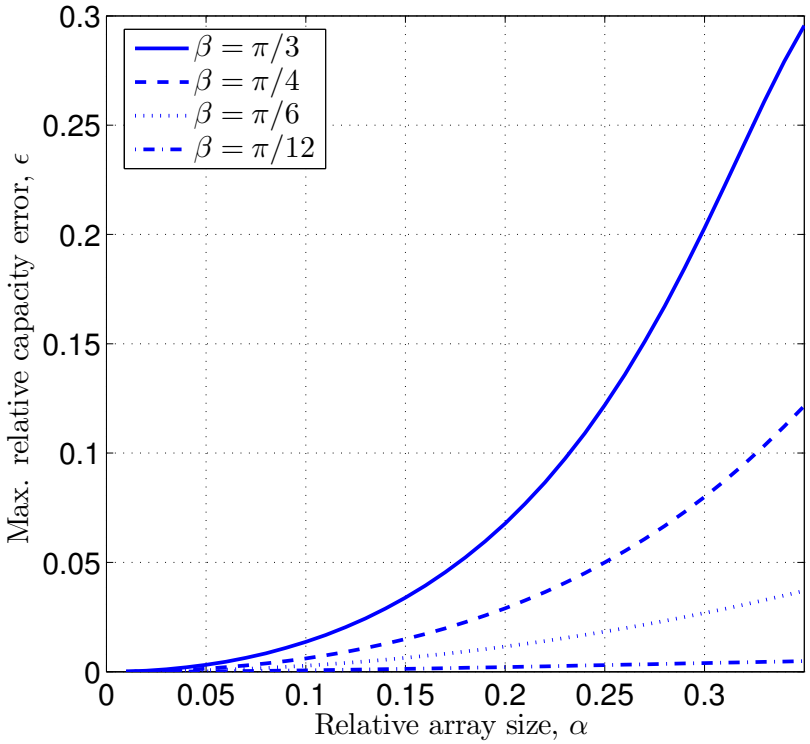

Fig. 8. Maximum ε (over ϕ_r) as a function of α for a 3×3 MIMO system with $\eta = 0$ dB, $\bar{\gamma} = 10$ dB, and different β.

Nevertheless, some general tendencies are possible to identify, and they will be explained through an example. For simplicity we define the quantities $\alpha = \frac{(N-1)d_t}{R} = \frac{(M-1)d_r}{R}$, which is the total array lengths relative to the Tx–Rx distance, and $\beta = \theta_t = \theta_r$.

In Figure 8, ε is plotted for a 3×3 MIMO system with $\bar{\gamma} = 10$ dB, as a function of α for different β and with $\eta = 0$ dB. ε is maximized over all values of ϕ_r. The figure indicates that an increase in α increases ε. This can be attributed to the fact that it increases the array sizes relative to the distance between them, which is negative with respect to the approximation accuracy as described earlier. Furthermore, an increase in β also increases ε. The explanation for this lies in the fact that when β increases, it decreases $\frac{\lambda}{R}$ in (24), which increases the sensitivity to distance errors with respect to phase errors in (9).

In Figure 9 we have plotted ε maximized with respect to ϕ_r as a function of $\bar{\gamma}$ for optimal design ($\eta = 0$ dB), both for the EP transmission case and the WF power allocation case. An intuitive explanation for the smaller ε in the WF case, is that the MI becomes less sensitive to the eigenvalues when we can adapt $\{\bar{\gamma}_i\}$. For large $\bar{\gamma}$, the ε for the two cases approach each other because the WF case approaches the EP transmission case.

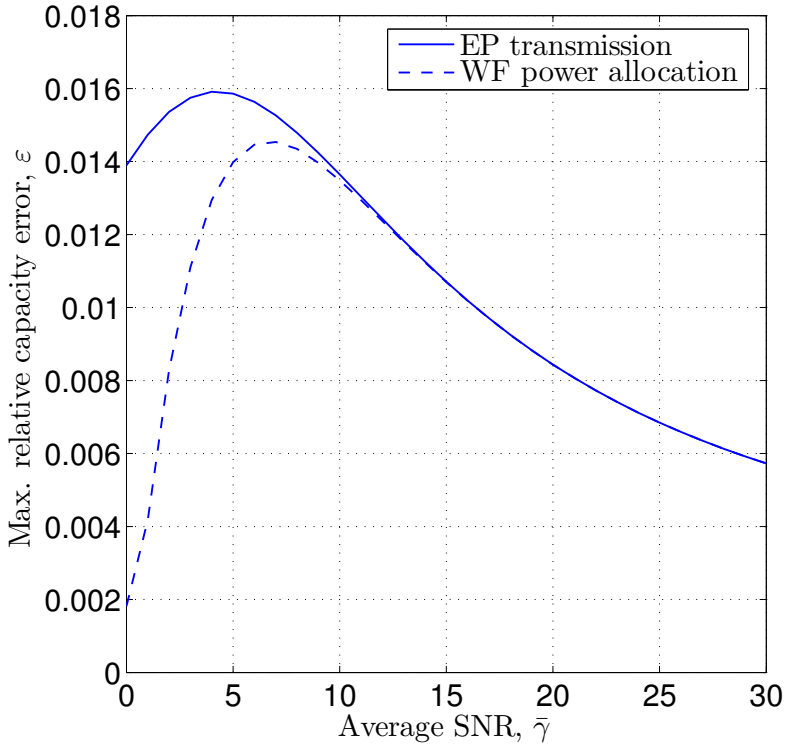

Fig. 9. Maximum ε (over ϕ_r) as a function of $\bar{\gamma}$ for a 3×3 MIMO system with $\eta = 0$ dB, $\alpha = 0.1$, and $\beta = \pi/3$.

APPENDIX II
OPTIMAL EIGENVALUES WITH RESPECT TO MI

From linear algebra theory we know that $\text{trace}(\mathbf{W}) = \sum_{i=1}^{U} \mu_i$ [20, p.92]. Because of the normalization of the channel matrix, the trace of $\mathbf{W}$ for the pure LOS case can easily be shown to be $N \cdot M = V \cdot U$, consequently

$$\sum_{i=1}^{U} \mu_i = UV. \tag{26}$$

When employing EP transmission, we need to maximize (2) using $\bar{\gamma}_i = \frac{\bar{\gamma}}{N}$ with respect to $\{\mu_i\}$, fulfilling the constraint given in (26). To do this we apply the method of *Lagrange multipliers* [20, p.228], and form the *Lagrangian*

$$\mathcal{L}_1 = \sum_{i=1}^{U} \ln\left(1 + \frac{\bar{\gamma}}{N}\mu_i\right) + \kappa\left(\sum_{i=1}^{U} \mu_i - UV\right). \tag{27}$$

From $\frac{\partial \mathcal{L}_1}{\partial \mu_i} = 0$ and (26), we have $U+1$ equations with $U+1$ unknowns. It can be shown

that $\frac{\partial \mathcal{L}_1}{\partial \mu_i} = 0$ gives

$$\mu_i = -\frac{\kappa N + \bar{\gamma}}{\kappa \bar{\gamma}}. \tag{28}$$

Using this in (26) we get

$$\kappa = -\frac{\bar{\gamma}}{N + V\bar{\gamma}}, \tag{29}$$

which we re-insert into (28) to obtain $\mu_i = V$. Thus, optimality is achieved when all eigenvalues are equal to V.

Next we investigate the case where the channel is known at the Tx as well, thus both μ_i and $\bar{\gamma}_i$ can be optimized. In this situation we maximize the MI from (2), both over $\{\mu_i\}$ and $\{\bar{\gamma}_i\}$, with the constraints given in (4) and (26). By looking at (2) it is obvious that when $N > U$, $\{\bar{\gamma}_i\}_{i=U+1}^{N} = 0$, thus we can write the constraint in (4) as a sum from 1 to U. The Lagrangian then becomes

$$\mathcal{L}_2 = \sum_{i=1}^{U} \ln\left(1 + \bar{\gamma}_i \mu_i\right) + \kappa_1 \left(\sum_{i=1}^{U} \mu_i - UV \right) + \kappa_2 \left(\sum_{i=1}^{U} \bar{\gamma}_i - \bar{\gamma} \right). \tag{30}$$

The $2U + 2$ equations with the $2U + 2$ unknowns are thus $\frac{\partial \mathcal{L}_2}{\partial \bar{\gamma}_i} = 0$, $\frac{\partial \mathcal{L}_2}{\partial \mu_i} = 0$, (4) and (26). Following a similar procedure as in the previous case we start with

$$\frac{\partial \mathcal{L}_2}{\partial \bar{\gamma}_i} = 0 \Rightarrow \bar{\gamma}_i = -\frac{\kappa_2 + \mu_i}{\kappa_2 \mu_i} \quad \text{and} \quad \frac{\partial \mathcal{L}_2}{\partial \mu_i} = 0 \Rightarrow \mu_i = -\frac{\kappa_1 + \bar{\gamma}_i}{\kappa_1 \bar{\gamma}_i}.$$

Combining these two equations we obtain

$$\bar{\gamma}_i = \frac{-1 \pm \sqrt{1 - 4\kappa_1 \kappa_2}}{2\kappa_2} \quad \text{and} \tag{31}$$

$$\mu_i = \frac{-1 \pm \sqrt{1 - 4\kappa_2 \kappa_1}}{2\kappa_1}. \tag{32}$$

Using these expressions in the constraints in (4) and (26), gives $\kappa_2 = -V\left(V\kappa_1 + 1\right)$ and $\kappa_1 = -\frac{\bar{\gamma}}{U}\left(\frac{\bar{\gamma}}{U}\kappa_2 + 1\right)$, which we can combine to get

$$\kappa_2 = -\frac{V}{1 + V\frac{\bar{\gamma}}{U}} \quad \text{and} \tag{33}$$

$$\kappa_1 = -\frac{\frac{\bar{\gamma}}{U}}{1 + V\frac{\bar{\gamma}}{U}}. \tag{34}$$

By investigating (31) and (32) together with the constraints, we find that the "+" sign in front

of the square root in these expressions gives a valid solution when $V\bar{\gamma}/N < 1$, while the "-" sign gives a valid solution when $V\bar{\gamma}/N > 1$. Utilizing this fact and (33) and (34) in (31) and (32), we reveal the result $\bar{\gamma}_i = \frac{\bar{\gamma}}{U}$ and $\mu_i = V$. Thus, as for the case of EP transmission, optimality with respect to the MI is achieved when all eigenvalues are equal to V.

APPENDIX III
CALCULATION OF LOS EIGENVALUES

The eigenvalues of the $\mathbf{W}$ matrix, in the pure LOS case, can be found based on the geometrical model presented in the beginning of Section III-A. We use $\mathbf{H} = \mathbf{H}_{\text{LOS}}$ ($K \to \infty$) in (3), and the relation [20, p.99]

$$\det\left(\mathbf{W} - \mathbf{I}_U \cdot \mu\right) = 0, \tag{35}$$

where $\det(\cdot)$ is the matrix determinant operator, to find the eigenvalues $\{\mu_i\}_{i=1}^{U}$. The authors have not been able to find analytical expressions for the eigenvalues in the case of exact path length from (7), therefore the approximate path length from (8) is used. The elements of $\mathbf{W}$, denoted $(\mathbf{W})_{k,l}$, are inner products between the rows ($M \leq N$) or columns ($M > N$) of $\mathbf{H}$, taking the form (cf. (13))

$$(\mathbf{W})_{k,l} = \frac{\sin\left(\frac{\pi}{\eta}(k-l)\right)}{\sin\left(\frac{\pi}{V\eta}(k-l)\right)} \exp\left[j\zeta_1(k-l)\right] \exp\left[j\zeta_2((k-1)^2 - (l-1)^2)\right]$$
$$k, l \in \{1, \ldots, U\}, \tag{36}$$

where ζ_1 and ζ_2 are different constants in the two cases ($M \leq N$ and $M > N$). The relation in (35) can be simplified by realizing that it can be written as

$$\det\left(\mathbf{B}\hat{\mathbf{W}}\mathbf{B}^H - \mathbf{I}_U \cdot \mu\right) = 0, \tag{37}$$

where $\mathbf{B}$ is a unitary diagonal matrix with diagonal elements

$$(\mathbf{B})_{k,k} = \exp\left(j\zeta_1 k\right) \exp\left(j\zeta_2(k-1)^2\right) \qquad k \in \{1, \ldots, U\}.$$

By multiplying (37) from the left with $\mathbf{B}^H$, and from the right with $\mathbf{B}$, we obtain an equivalent expression for the same eigenvalues, $\det\left(\hat{\mathbf{W}} - \mathbf{I}_U \cdot \mu\right) = 0$. Thus, the eigenvalues of the Hermitian matrix $\mathbf{W}$ are the same as for the symmetric Toeplitz matrix $\hat{\mathbf{W}}$, with elements

$$(\hat{\mathbf{W}})_{k,l} = \frac{\sin\left(\frac{\pi}{\eta}(k-l)\right)}{\sin\left(\frac{\pi}{V\eta}(k-l)\right)} \qquad k,l \in \{1,\ldots,U\}. \tag{38}$$

The eigenvalues can be calculated by a mathematical application such as e.g. *Mathematica*, but the expressions becomes long for large values of U. The eigenvalues for $U = 2$ and $U = 3$ are given in (18) and (19)-(21) respectively, calculated by using the *Eigenvalues* command in *Mathematica*, and simplified by trigonometric relations [20, pp.127-128].

REFERENCES

[1] G. J. Foschini and M. J. Gans, "On limits of wireless communications in fading environment when using multiple antennas," *Wireless Pers. Commun.*, vol. 6, pp. 311–335, March 1998.

[2] E. Telatar, "Capacity of multiantenna Gaussian channels," *AT&T Bell Laboratories, Tech. Memo*, June 1995.

[3] T. Kaiser, "When will smart antennas be ready for the market? Part I," *IEEE Sig. Proc. Mag.*, vol. 22, pp. 87–92, March 2005.

[4] ——, "When will smart antennas be ready for the market? Part II - Results," *IEEE Sig. Proc. Mag.*, vol. 22, pp. 174–176, Nov. 2005.

[5] D. Gesbert, M. Shafi, D.-S. Shiu, P. J. Smith, and A. Naguib, "From theory to practice: An overview of MIMO space-time coded wireless systems," *IEEE J. Select. Areas Commun.*, vol. 21, no. 3, pp. 281–302, April 2003.

[6] P. F. Driessen and G. Foschini, "On the capacity formula for multiple input-multiple output wireless channels: A geometric interpretation," *IEEE Trans. Commun.*, vol. 47, no. 2, pp. 173–176, Feb. 1999.

[7] D. Gesbert, H. Bölcskei, D. A. Gore, and A. J. Paulraj, "Outdoor MIMO wireless channels: Models and performance prediction," *IEEE Trans. Commun.*, vol. 50, no. 12, pp. 1926–1934, Dec. 2002.

[8] T. Haustein and U. Krüger, "Smart geometrical antenna design exploiting the LOS component to enhance a MIMO system based on Rayleigh-fading in indoor scenarios," in *Proc. IEEE PIMRC*, Beijing, China, Sep. 2003, pp. 1144–1148.

[9] I. Sarris and A. R. Nix, "Maximum MIMO capacity in line-of-sight," in *Proc. IEEE ICICS*, Bangkok, Thailand, Dec. 2005, pp. 1236–1240.

[10] A. A. Hutter, F. Platbrood, and J. Ayadi, "Analysis of MIMO capacity gains for indoor propagation channels with LOS component," in *Proc. IEEE PIMRC*, Lisbon, Portugal, Sep. 2002, pp. 1337–1347.

[11] J.-S. Jiang and M. A. Ingram, "Spherical wave model for short-range MIMO," *IEEE Trans. Commun.*, vol. 53, no. 9, pp. 1534–1541, Sept. 2005.

[12] F. Bøhagen, P. Orten, and G. E. Øien, "Design of capacity-optimal high-rank line-of-sight MIMO channels," *IEEE Trans. Wireless Commun.*, vol. 6, no. 3, March 2007 *Available from: http://www.unik.no/personer/frodbo/*.

[13] ——, "Construction and capacity analysis of high-rank line-of-sight MIMO channels," in *Proc. IEEE WCNC*, New Orleans, USA, March 2005, pp. 432–437.

[14] I. Sarris and A. R. Nix, "Design and performance assessment of maximum capacity MIMO architectures in line-of-sight," *IEE Proc. in Commun.*, vol. 153, no. 4, pp. 482–488, Aug. 2006.

[15] H. Xu, M. J. Gans, N. Amitay, and R. A. Valenzuela, "Experimental verification of MTMR system capacity in controlled propagation environment," *Electronic letters*, vol. 37, no. 15, pp. 936–937, July 2001.

[16] I. Sarris, A. R. Nix, and A. Doufexi, "High-throughput multiple-input multiple-output systems for in-home multimedia streaming," vol. 13, no. 5, pp. 60–66, Oct. 2006.

[17] I. Sarris, A. Nix, and M. Beach, "Capacity evaluation of LOS-optimized and standard MIMO antenna arrays at 5.2 GHz," in *COST 2100 TD(07) 058*, Lisbon, Portugal, Feb. 2007.

[18] F. Bøhagen, P. Orten, and G. E. Øien, "Modeling and analysis of 40 GHz MIMO system for fixed wireless access," in *Proc. IEEE VTC*, Stockholm, Sweden, May 2005.

[19] G. L. Stüber, *Principles of Mobile Communication*, 2nd ed. Kluwer Academic Publishers, 2001.

[20] L. Råde and B. Westergren, *Mathematics Handbook for Science and Engineering*, 5th ed. Springer, 2004.

[21] IEEE 802.16-2004, “IEEE standard for local and metropolitan area networks part 16: Air interface for fixed broadband wireless access systems,” Oct. 2004.

[22] S. L. Loyka, “Channel capacity of MIMO architecture using the exponential correlation matrix,” *IEEE Commun. Letters*, vol. 5, no. 9, pp. 369–371, Sep. 2001.

[23] G. L. Turin, “On optimal diversity reception,” *IRE Trans. Commun. Syst.*, vol. 10, no. 1, pp. 22–31, March 1962.